ADVANCES IN ATMOSPHERIC SCIENCES, VOL. 31, SEPTEMBER 2014, 1221–1232

Effects of Additional HONO Sources on Visibility over the North China Plain

LI Ying[1], AN Junling*[1], and Ismail GULTEPE[2]

[1]*State Key Laboratory of Atmospheric Boundary Layer Physics and Atmospheric Chemistry, Institute of Atmospheric Physics, Chinese Academy of Sciences, Beijing* 100029

[2]*Cloud Physics and Severe Weather Research Section, Environment Canada, Toronto, Ontario M3H 5T4, Canada*

(Received 25 January 2014; revised 3 March 2014; accepted 5 March 2014)

ABSTRACT

The objective of the present study was to better understand the impacts of the additional sources of nitrous acid (HONO) on visibility, which is an aspect not considered in current air quality models. Simulations of HONO contributions to visibility over the North China Plain (NCP) during August 2007 using the fully coupled Weather Research and Forecasting/Chemistry (WRF/Chem) model were performed, including three additional HONO sources: (1) the reaction of photo-excited nitrogen dioxide (NO_2^*) with water vapor; (2) the NO_2 heterogeneous reaction on aerosol surfaces; and (3) HONO emissions. The model generally reproduced the spatial patterns and diurnal variations of visibility over the NCP well. When the additional HONO sources were included in the simulations, the visibility was occasionally decreased by 20%–30% (3–4 km) in local urban areas of the NCP. Monthly-mean concentrations of NO_3^-, NH_4^+, SO_4^{2-} and $PM_{2.5}$ were increased by 20%–52% (3–11 $\mu g\ m^{-3}$), 10%–38%, 6%–10%, and 6%–11% (9–17 $\mu g\ m^{-3}$), respectively; and in urban areas, monthly-mean accumulation-mode number concentrations (AMNC) and surface concentrations of aerosols were enhanced by 15%–20% and 10%–20%, respectively. Overall, the results suggest that increases in concentrations of $PM_{2.5}$, its hydrophilic components, and AMNC, are key factors for visibility degradation. A proposed conceptual model for the impacts of additional HONO sources on visibility also suggests that visibility estimation should consider the heterogeneous reaction on aerosol surfaces and the enhanced atmospheric oxidation capacity due to additional HONO sources, especially in areas with high mass concentrations of NO_x and aerosols.

Key words: HONO, visibility, aerosols, WRF/Chem, North China Plain

Citation: Li, Y., J. L. An, and I. Gultepe, 2014: Effects of additional HONO sources on visibility over the North China Plain. *Adv. Atmos. Sci.*, **31**(5), 1221–1232, doi: 10.1007/s00376-014-4019-1.

1. Introduction

The importance of nitrous acid (HONO) in issues related to tropospheric photochemistry has risen in recent years because of its significant contribution to the hydroxyl radical (OH), which is the key oxidant in the atmosphere (Alicke et al., 2002). Nevertheless, the formation mechanisms of HONO and the strength of its sources remain uncertain. Among known HONO chemical sources, the chemistry of electronically excited NO_2 and H_2O ($NO_2^* + H_2O \rightarrow$ HONO + OH; hereafter referred to as NO_2^* chemistry) (Crowley and Carl, 1997; Li et al., 2008; Amedro et al., 2011) has received much attention in recent years for its implication in the enhancement of OH. Studies conclude that the impact of NO_2^* chemistry on air quality is more significant over urban and coastal areas with high NO_x (= NO + NO_2) emissions, while it is minor in rural and background areas where NO_x emissions are relatively low (Wennberg and Dabdub, 2008; Sarwar et al., 2009; Ensberg et al., 2010; An et al., 2011; Li et al., 2011; Jorba et al., 2012; An et al., 2013; Zhang et al., 2013). The maximum enhancement of surface ozone (O_3) concentrations due to the NO_2^* chemistry identified in eastern Asia under contemporary emissions are more than 30 ppbv (Li et al., 2011; Jorba et al., 2012). NO_2^* chemistry also notably affects mass concentrations of fine particles. During a typical summer episode over the South Coast Air Basin of California, mass concentrations of particulate matter with diameter $\leqslant 2.5$ μm ($PM_{2.5}$) and nitrate (NO_3^-) near Riverside were enhanced by up to 20 $\mu g\ m^{-3}$ and 25%, respectively (Wennberg and Dabdub, 2008; Ensberg et al., 2010). Some of the earlier studies performed over eastern Asia also showed that monthly-mean daytime NO_3^- concentrations were increased by as much as 7% over the North China Plain (NCP) during August 2007 (An et al., 2013) when the NO_2^* chemistry was inserted into a fully coupled Weather Research and Forecasting/Chemistry (WRF/Chem) model (Grell et al., 2005; Fast et al., 2006). These works show the potentially important effects of NO_2^* chemistry on the air quality of areas with high NO_x emissions.

Another HONO source receiving considerable attention is the NO_2 heterogeneous reaction ($2NO_2 + H_2O \rightarrow HNO_3$

* Corresponding author: AN Junling
Email: anjl@mail.iap.ac.cn

+ HONO), which is believed to be the most important formation pathway of nocturnal HONO (Kleffmann et al., 1998; Finlayson-Pitts et al., 2003). Recent studies have reported that heterogeneous NO_2 hydrolysis can increase $PM_{2.5}$ concentrations by more than 10%, and the enhancements are attributable mainly to increased NO_3^- and ammonium (NH_4^+) concentrations, albeit with slight increases also found in sulfate (SO_4^{2-}) and secondary organic aerosols (SOA) (Gonçalves et al., 2012; An et al., 2013).

The significant contribution of HONO sources to aerosol concentrations (for hydrophilic particles, e.g., SO_4^{2-}, NO_3^-, and NH_4^+) addresses the question of the relative contribution of HONO sources to visibility. Excluding rainy and foggy conditions (Gultepe et al., 2007, 2009), the dominant factor causing visibility degradation is aerosols (Chang et al., 2009; Chen et al., 2012). The NCP, a region with heavy aerosol loadings (Zhao et al., 2006; Yang et al., 2011), is one of the most populated and polluted areas of the world, suffering severely low visibility conditions in recent times. Excluding days of precipitation and fog, the annual mean visibility from 1999 to 2007 in Beijing was reported to have fallen to between 10 and 15 km, with a mean value of below 10 km in summer, the season with the lowest visibility (Zhang et al., 2010).

It has been shown previously that the low visibility over the NCP is primarily caused by the high mass burden of $PM_{2.5}$, with sulfate and nitrate as the major contributors to the total extinction coefficient (Quan et al., 2011; Cao et al., 2012; Han et al., 2013). For example, $(NH_4)_2SO_4$ and NH_4NO_3 contributed 67% to the total extinction during the 2006 Campaign of Air Quality Research in Beijing (CAREBeijing-2006) (Jung et al., 2009).

The main purpose of this work is to evaluate the impacts of additional HONO sources on visibility, and explore the key factors of visibility degradation due to HONO sources, which are aspects that have not been studied previously in any great detail. In this work, besides HONO gas-phase production from OH and NO, three additional HONO sources (NO_2^* chemistry, the NO_2 heterogeneous reaction on aerosol surfaces, and HONO emissions) coupled into the WRF/Chem model were used to simulate the contributions of HONO to the prediction of visibility over the NCP during August 2007. The model and observations are described in section 2. Section 3 gives an evaluation of the model simulations and discusses how the additional HONO sources impact visibility, and then proposes a conceptual model for the effects of HONO sources on visibility prediction. The conclusions of the study are presented in section 4.

2. Method

2.1. *Model set up*

Version 3.2.1 of the WRF/Chem model (Grell et al., 2005; Fast et al., 2006) has been updated to include three additional HONO sources (Li et al., 2011; An et al., 2011, 2013). The NO_2^* chemistry was added into the Carbon-Bond Mechanism Z (CBM-Z) (Zaveri and Peters, 1999) gas-phase chemical mechanism. The rate constant for the reaction of NO_2^* with H_2O was estimated as 9.1×10^{-14} cm^3 molecule^{-1} s^{-1} (Li et al., 2011). HONO heterogeneous formation on aerosol surfaces followed the recommendations of Jacob (2000), where the total aerosol surface (S_a) per volume of air is one of the key factors for computing the reaction rate. In this study, S_a was derived from aerosol mass concentrations and the number density in each bin set by the Model for Simulating Aerosol Interactions and Chemistry (MOSAIC) (Zaveri et al., 2008), which was fully coupled in the WRF/Chem (Fast et al., 2006). Eight bins for the aerosol size distribution were employed (Table 1). Aerosols in MOSAIC were composed of SO_4^{2-}, NO_3^-, NH_4^+, chloride, sodium, other unspecified inorganics, organic carbon, elemental carbon, and water.

HONO direct emissions were estimated as 0.8% for the HONO/NO_x emission ratio (Kurtenbacha et al., 2001). Besides direct emissions, HONO emissions in this study also included 2.3% of the NO_x emitted in diesel exhaust converted to HONO via the heterogeneous reaction with semivolatile organics (Gutzwiller et al., 2002). The final ratio for HONO/NO_x as HONO emissions was computed as 1.18% in the urban center of Beijing (Li et al., 2011; An et al., 2013).

For the WRF/Chem configuration, three nested domains were employed, with the third domain covering the NCP (Fig. 1). The finest horizontal resolution was 9 km, with 28 levels ranging from the surface to ~50 hPa. Initial and boundary conditions for meteorological fields were obtained from the US National Centers for Environmental Prediction (NCEP) analysis data applied to nudging every 6 h, and those for chemical fields were constrained every 6 h from the outputs of the Model for Ozone and Related chemical Tracers, version 4 (MOZART-4) (Emmons et al., 2010). Monthly anthropogenic emissions used in this study were derived from Zhang et al. (2009).

The detailed physical and chemical schemes for the simulations can be found in Li et al. (2011). An evaluation of the updated model has been conducted for the NCP during August 2007 (Li et al., 2011), in which it was stated that simulations of HONO, O_3 and NO_x concentrations were improved when the additional HONO sources were considered. Diurnal variations of $PM_{2.5}$ and PM_{10} concentrations were satisfactorily reproduced. The simulated aerosol number (N_a) and S_a

Table 1. Aerosol dry diameter range for the eight size bins employed by MOSAIC (Fast et al., 2006).

Bin	Lower diameter (μm)	Upper diameter (μm)
1	0.0390625	0.078125
2	0.078125	0.15625
3	0.15625	0.3125
4	0.3125	0.625
5	0.625	1.25
6	1.25	2.5
7	2.5	5.0
8	5.0	10.0

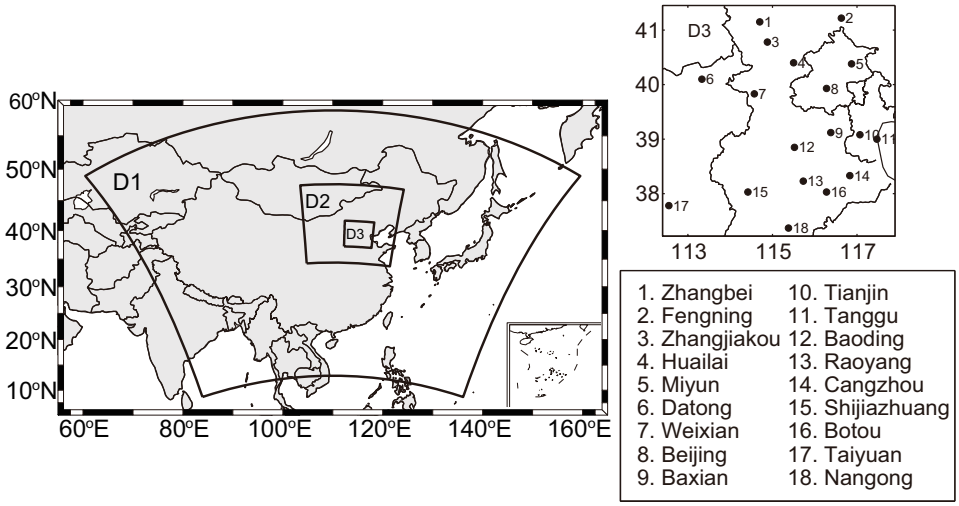

Fig. 1. Modeling domains and meteorological stations providing the observed visibility data.

were found to be within the observed range (Li et al., 2011; An et al., 2013; Tang et al., 2014).

2.2. *Visibility prediction*

One of the important objectives of this paper is to evaluate the model's performance in predicting atmospheric visibility. Daytime visibility ($V_{\rm d}$) can be calculated by the Koschmieder equation (Koschmieder, 1924):

$$V_{\rm d} = -\ln(\varepsilon)/\beta_{\rm ext}\ , \tag{1}$$

where $\beta_{\rm ext}$ is the extinction coefficient and ε is the brightness contrast threshold assumed as 0.02 in this work (Gultepe et al., 2006). The MOSAIC aerosol module calculated the aerosol $\beta_{\rm ext}$ based on Mie theory (Ackerman and Toon, 1981; Barnard et al., 2010), and values at 550 nm were adopted in this study.

Nighttime visibility ($V_{\rm n}$) was obtained using the simplified Allard's law (Gultepe et al., 2008):

$$V_{\rm n} = \frac{I_0}{C_{\rm DB}} e^{-\beta_{\rm ext} V_{\rm n}}\ , \tag{2}$$

where $C_{\rm DB} = 0.084$ miles^{-1} and $I_0 = 25$ candela. Comparing Eqs. (1) and (2), a simplified equation for the relationship of $V_{\rm d}$ and $V_{\rm n}$ was given by Gultepe et al. (2008):

$$V_{\rm n} = 1.8507 V_{\rm d}^{0.814}\ . \tag{3}$$

2.3. *Observations*

The observed visibility data were collected at more than 600 meteorological stations in China. Those stations located on the NCP are shown in Fig. 1(D3). Visibility was observed by trained observers under standard procedures of the Chinese Meteorological Administration (Chang et al., 2009; Lin et al., 2012). Observations were available at local times of 0200, 0800, 1400 and 2000, except for the stations of Zhangbei, Datong, Taiyuan, Fengning, Miyun, Tianjin and Raoyang, which conduct hourly visibility observations. In this study, observations during periods of precipitation or relative humidity (RH) exceeding 90% were discarded (Mebust et al., 2003; Chang et al., 2009) to prevent hydrometeors from biasing the evaluation.

The HONO concentrations were measured by Differential Optical Absorption Spectroscopy (DOAS) at the Meteorological Tower (39.8°N, 116.3°E) in Beijing during August of 2007 (Zhu et al., 2009). Observed hourly concentrations of O_3, $PM_{2.5}$ and PM_{10} across the NCP were taken from the Beijing Atmospheric Environmental Monitoring Action (Li et al., 2011). Daily-mean concentrations of SO_4^{2-}, NO_3^-, and NH_4^+ were measured at Peking University (40.0°N, 116.3°E) during 2–31 August 2007 as part of the CAREBeijing-2007 Experiment (Ianniello et al., 2011).

2.4. *Simulations*

Five simulations were conducted in this study. The first one was a "reference case" (Case R), which was performed using the standard CBM-Z mechanism and the MOSAIC module. The other three cases included the NO_2^* chemistry, NO_2 heterogeneous reaction on aerosol surfaces, and HONO emissions, respectively. The last simulation, called the "enhanced case" (Case E) included all of the three HONO sources. Sensitivity simulations were performed for 1–31 August 2007 with a spin-up period of seven days.

3. Results and discussion

3.1. *Impacts of additional HONO sources on visibility*

An evaluation of the WRF/Chem model in terms of the spatial pattern of monthly-mean visibility at 1400 LST (local standard time) is shown in Fig. 2. The visibility observations ranged from 9 km to 29 km across the NCP during August 2007; visibility was down to < 15 km in the south. The simulated values of visibility were 2–7 km larger than observations in the south of the NCP. Apart from its overestimation in the southern region, the WRF/Chem model generally repro-

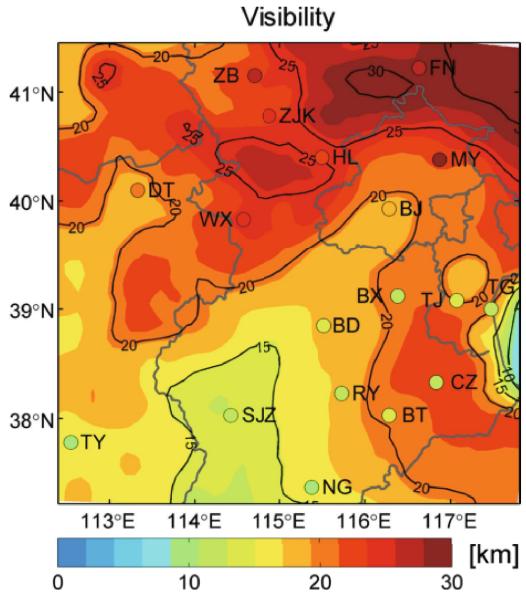

Fig. 2. Monthly-mean visibility simulations for the reference case and observations at 1400 LST August 2007. Station observations over the NCP are indicated by colored circles.

duced the observed regional-scale pattern well (Fig. 2). The mean observed and simulated visibility, mean bias (MB), normal mean bias (NMB), normal mean error (NME), and correlation coefficient (RC) were 17 km, 20 km, 2.6 km, 15%, 24%, and 0.74, respectively. Hourly visibility comparisons at urban sites are shown in Fig. 3. The observed visibility is relatively good in the afternoon because the higher temperatures reduce the RH. The higher planetary boundary layer height also provides suitable conditions for vertical mixing of pollutants, leading to improved visibility. The WRF/Chem simulations captured the trend of diurnal variations and magnitudes of the observed visibility. The simulated mean visibility at the seven urban sites was 10.9 km, very close to the observed mean value of 11.1 km.

When the NO_2^* chemistry, the NO_2 heterogeneous reaction on aerosol surfaces, and HONO emissions were considered in the simulations, visibility at 1400 LST was decreased by up to 20%–30% (3–4 km) during August 2007 in local urban areas (Fig. 4a). Inclusion of the additional HONO sources led to improvements in the visibility simulations. The simulated mean visibility, MB, NMB, and NME for the meteorological stations shown in Fig. 2 were 19.5 km, 2.1 km, 12%, and 22%, respectively. Figure 4a also shows the maximum percentage decreases of 40%–55% were located over Bohai Bay (to the east of Tianjin). The shallow marine boundary layer and abundant moisture over the Bohai Sea are favorable for the NO_2 heterogeneous reaction and NO_2^* chemistry (Sarwar et al., 2009; Jorba et al., 2012; An et al., 2013). Up to 10% (1–2 km) decreases in visibility were

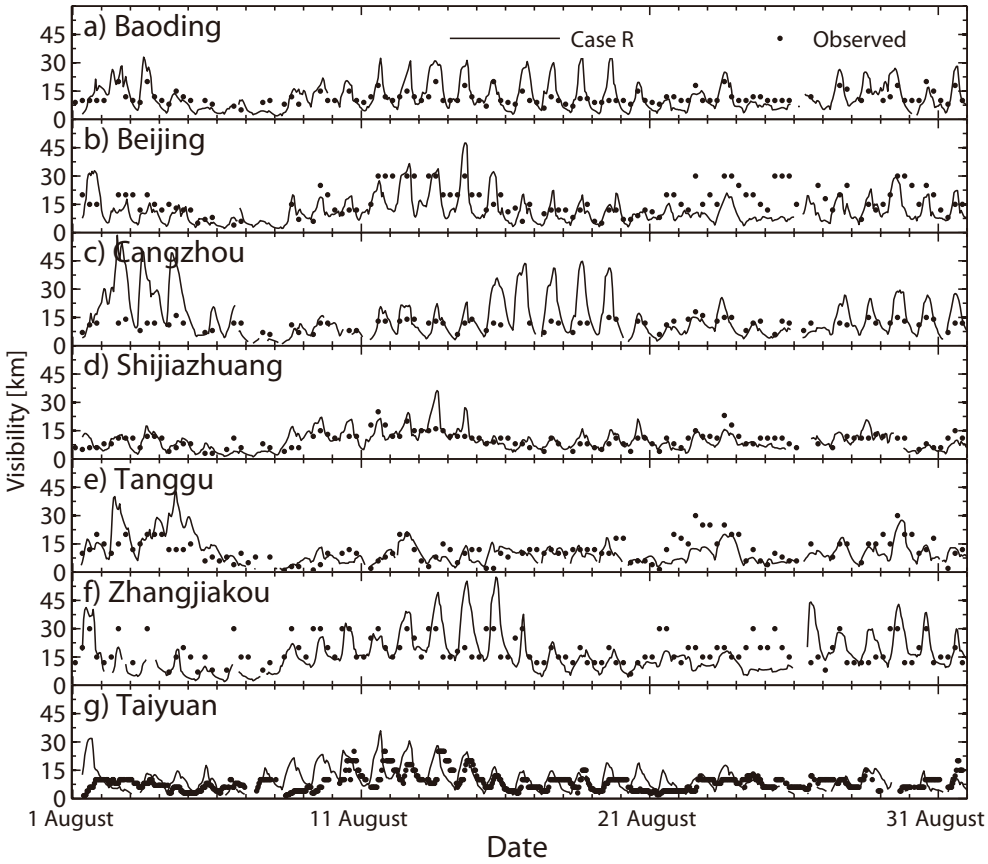

Fig. 3. Simulated and observed visibility at urban stations of the NCP in August 2007.

found in the rural areas (Fig. 4a).

Among the three HONO sources, the NO_2 heterogeneous reaction was the largest contributor to the visibility degradation, with 10%–20% decreases in urban areas and 20%–30% decreases over Bohai Bay. The NO_2^* chemistry resulted in 4%–10% decreases in visibility over local polluted regions and 8%–10% decreases along Bohai Bay. The contribution of HONO emissions to visibility was minor, with less than 6% reductions in urban areas (not shown). Figure 4b shows the enhancements of monthly-mean total aerosol β_{ext} near the ground due to the three additional HONO sources. Increases of 10%–21% β_{ext} were found in Beijing, Tianjin, south of Hebei Province, and Bohai Bay. Accordingly, the values of monthly-mean visibility decreased by 2%–6% (0.5–1 km) over the NCP during August 2007.

3.2. *Key factors for visibility changes due to additional HONO sources*

The dominant factor causing visibility degradation under cloud- and fog-free conditions is aerosols. Specifically, the aerosol mass concentration, chemical composition, and size distribution are important parameters affecting visibility (Cheng et al., 2008; Jung et al., 2009; Deng et al., 2011; Han et al., 2013). In the following sections, we summarize the effects of additional HONO sources on aerosol mass concentrations and aerosol sizes.

3.2.1. *Impacts of additional HONO sources on aerosol mass concentrations*

In this section we first discuss the temporal evolution of HONO, O_3, PM_{10}, and the main inorganic components of PM_{10} in Beijing. These results are shown in Fig. 5. Coupling additional HONO sources into the model significantly improved HONO simulations compared to the reference case (Fig. 5a). The mean values were enhanced from 0.08 ppb to 1.12 ppb; and the MB, NMB, and NME changed from −0.94 ppb, −92% and 92% to 0.29 ppb, 29%, and 56%, respectively. These results are comparable to the results of An et al. (2013).

The enhanced HONO concentrations as well as the NO_2^* chemistry increased OH concentrations in the boundary layer, thus enhanced O_3 production, especially for its peak values (Wennberg and Dabdub, 2008; Li et al., 2011). As shown in Fig. 5b, the maximum O_3 increases (10–21 ppb) due to the additional HONO sources largely occurred around noon. An increase in OH and O_3 concentrations as well as the NO_2 heterogeneous reaction on aerosol surfaces can further enhance particulate matter production (An et al., 2013). The simulated mean NO_3^- and NH_4^+ changed from 19.3 μg m^{-3} and 8.5 μg m^{-3} to 25.3 μg m^{-3} and 10.3 μg m^{-3}, respectively. Increases in NO_3^- and NH_4^+ concentrations largely contributed to increases of PM_{10} (Figs. 5c–f). Enhancements of $PM_{2.5}$ concentrations due to the three additional HONO sources were also found over the NCP region. As shown in Fig. 6, the maximum increase of $PM_{2.5}$ concentrations at the monitoring stations of Baoding (38.9°N, 115.5°E), Cangzhou (38.3°N, 116.8°E), Shijiazhuang (38.0°N, 114.5°E) and Tangshan (39.6°N, 118.2°E) were 49.6 μg m^{-3} (16.2%), 73.0 μg m^{-3} (27.5%), 44.0 μg m^{-3} (16.9%) and 81.9 μg m^{-3} (44.0%), respectively.

Percentage increases in monthly-mean concentrations of NO_3^-, NH_4^+, SO_4^{2-}, and $PM_{2.5}$ over the NCP due to the additional HONO sources are shown in Fig. 7. Remarkable enhancements were found in both NO_3^- and NH_4^+ concentrations. NO_3^- and NH_4^+ in the polluted areas increased by 20%–52% (3–11 μg m^{-3}) and 10%–38% (1–4 μg m^{-3}), respectively. SO_4^{2-} concentrations were enhanced by 6%–10%. The NO_3^-, NH_4^+ and SO_4^{2-} enhancements were largely re-

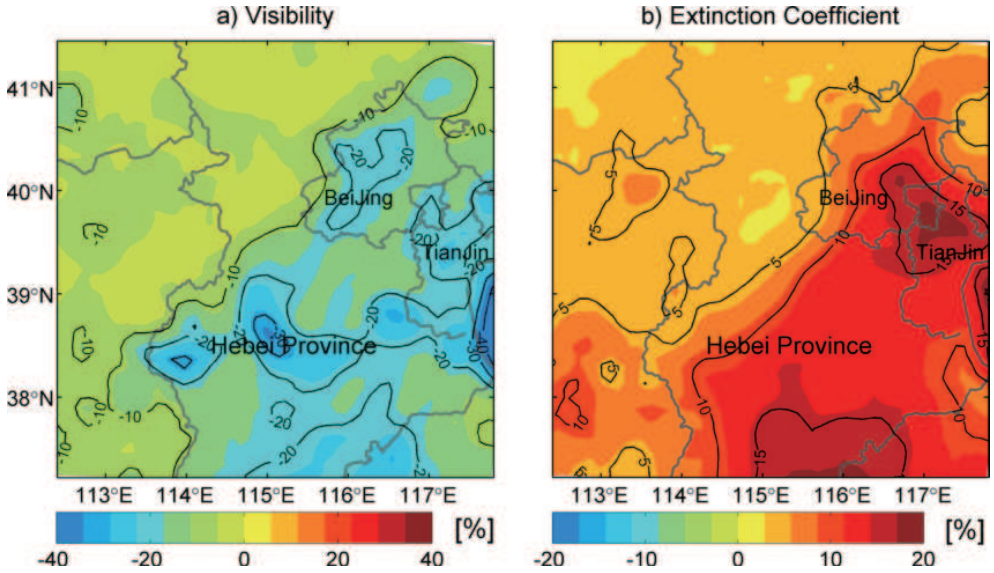

Fig. 4. (a) Maximum changes of visibility at 1400 LST and (b) enhancements of monthly-mean total aerosol extinction coefficients over the NCP in August 2007 due to the inclusion of NO_2^* chemistry, the NO_2 heterogeneous reaction on aerosol surfaces, and HONO emissions.

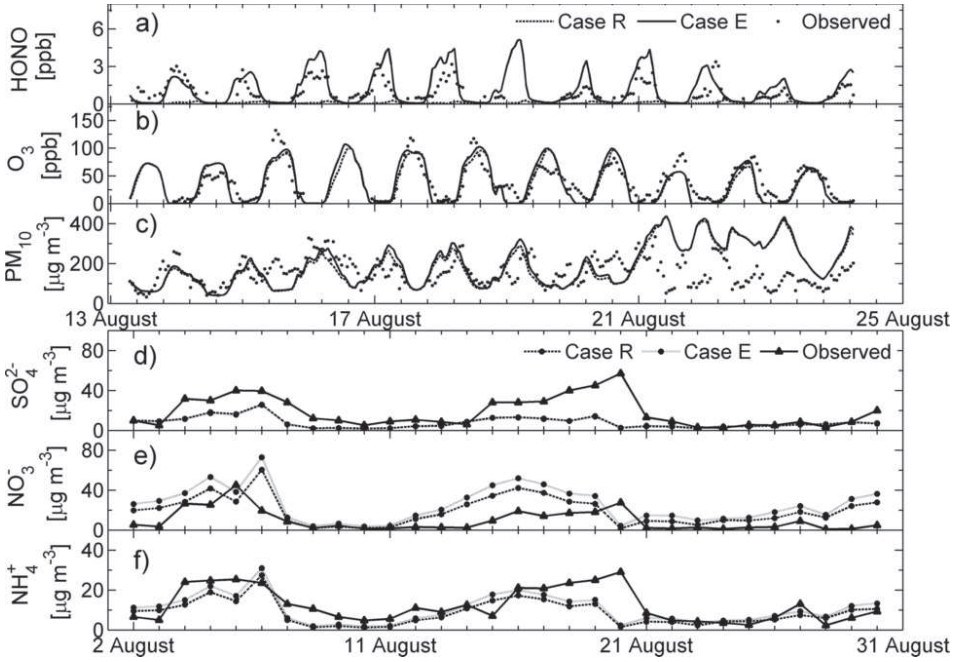

Fig. 5. Comparison of simulated HONO, O_3, PM_{10}, SO_4^{2-}, NO_3^- and NH_4^+ concentrations with observations in Beijing. Measurements of HONO, O_3 and PM_{10} were taken at the Meteorological Tower and those of sulfate, nitrate and ammonium concentrations were performed at Peking University in August 2007 (Ianniello et al., 2011).

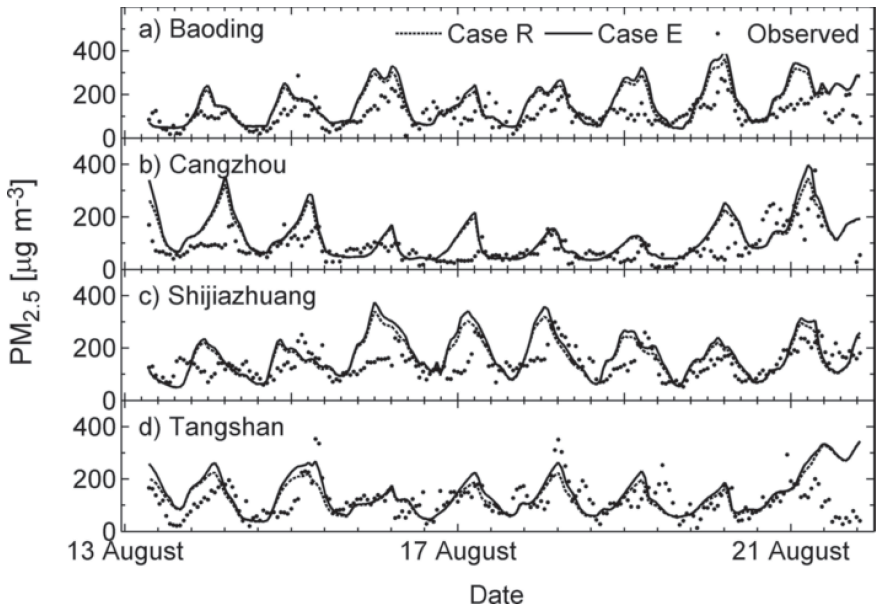

Fig. 6. Simulated and measured $PM_{2.5}$ concentrations (units: μg m^{-3}) at the stations of Baoding, Cangzhou, Shijiazhang and Tangshan, which are located in urban areas of the NCP. Case R is a reference case; Case E includes NO_2^* chemistry, the NO_2 heterogeneous reaction on aerosol surfaces, and HONO emissions.

sponsible for $PM_{2.5}$ increases. Up to 17 μg m^{-3} (11%) increases in $PM_{2.5}$ concentrations were found in the southern NCP (Fig. 7d).

The increment of nitrate due to the additional HONO sources was related to the enhanced OH level. As shown in Fig. 7e, the monthly-mean concentrations of OH were increased by 20%–40% over Beijing, Tianjin and south of Hebei Province. The enhanced OH as well as the NO_2 heterogeneous reaction resulted in the enhancements of HNO_3 (Fig. 7f). Gas phase HNO_3 could then partition into the aerosol phase, or be absorbed onto existing aerosols to form NO_3^-. The HONO-related enhancement of ammonium was largely

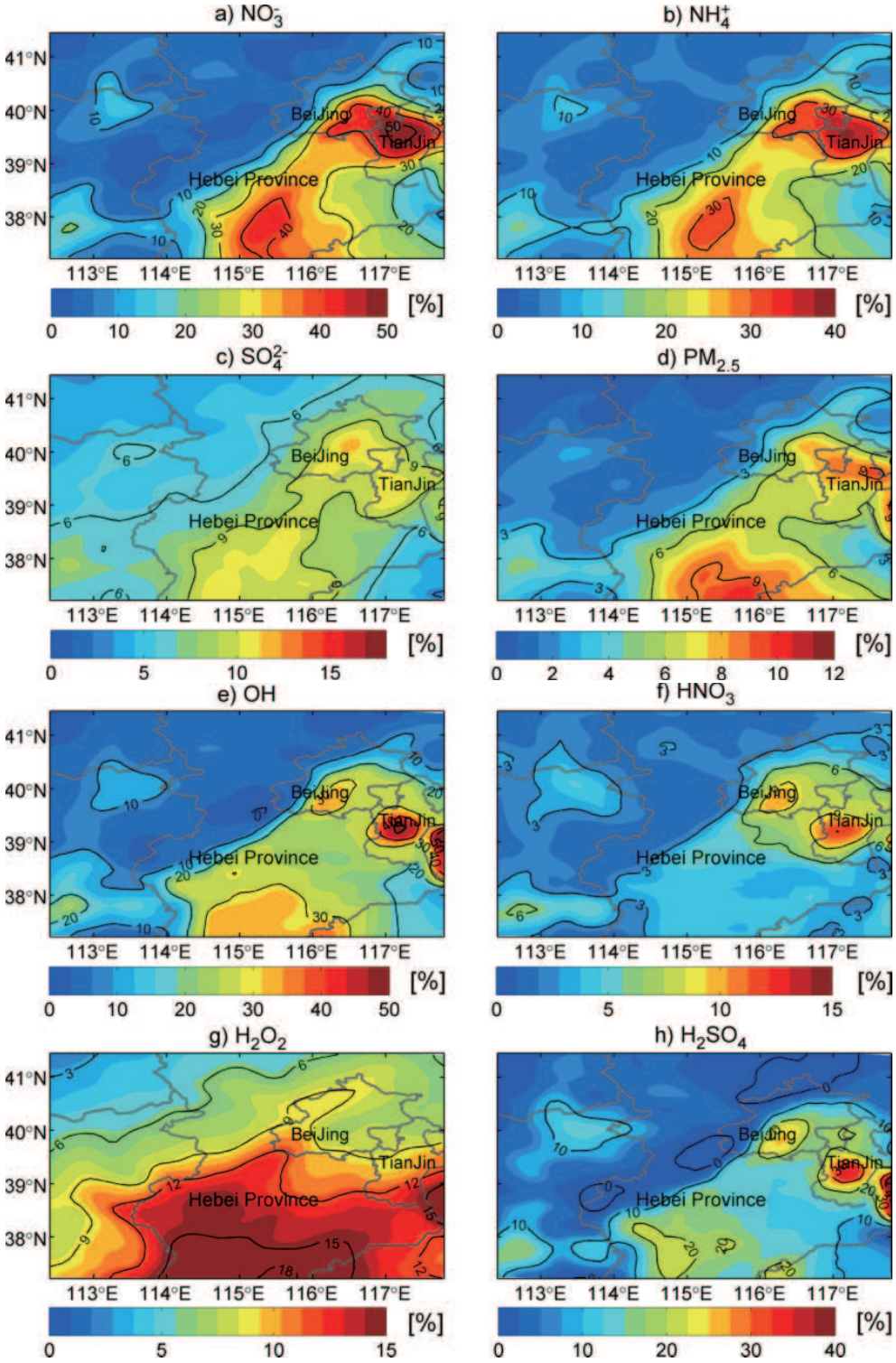

Fig. 7. Percentage increases of monthly-mean concentrations of (a) NO_3^-, (b) NH_4^+, (c) SO_4^{2-}, (d) $PM_{2.5}$, (e) OH, (f) HNO_3, (g) H_2O_2, and (h) H_2SO_4 over the NCP during August 2007 due to the inclusion of NO_2^* chemistry, the NO_2 heterogeneous reaction on aerosol surfaces, and HONO emissions.

due to the increases in HNO_3 and H_2SO_4 (Figs. 7f and h) that could be neutralized by NH_3 to form NH_4^+. The enhanced H_2SO_4 could also condense to form SO_4^{2-}. In addition, the increment of SO_4^{2-} due to the additional HONO sources may have been mainly related to the enhanced H_2O_2 (Fig. 7g) that depended indirectly on the OH concentrations. The aqueous-phase oxidation of dissolved SO_2 is considered to be the main source of SO_4^{2-}, with H_2O_2 being the most effective oxidant followed by O_3 (Ianniello et al., 2011). Therefore, the increased H_2O_2 and O_3 due to the additional HONO sources

contributed to the SO_4^{2-} enhancements. The HONO-related enhancements of $PM_{2.5}$ and its main inorganic components presented in this study are consistent with previous studies conducted in Mexico City (Li et al., 2010) and Madrid, Spain (Gonçalves et al., 2012). Elshorbany et al. (2014) recently conducted a global simulation of HONO effects and the results showed that NO_3^-, NH_4^+ and SO_4^{2-} were significantly enhanced, especially in regions that are rich in both NO_x and ammonia, e.g., eastern China.

The additional HONO sources also increased daily aerosol mass concentrations. The maximum daily-mean enhancements of NO_3^- and NH_4^+ during August 2007 were up to 100% in urban areas. The largest enhancements of daily mean SO_4^{2-} and $PM_{2.5}$ were about 10%–40% and 5%–22%, respectively (not shown). The significant increases in hourly, daily and monthly mean concentrations of $PM_{2.5}$ and its hydrophilic components indicate that the additional HONO sources can reduce visibility through enhancing aerosol concentrations, particularly for NO_3^- and SO_4^{2-}. These are identified as the main aerosol components contributing to the total extinction over the NCP (Jung et al., 2009; Han et al., 2013).

3.2.2. *Impacts of additional HONO sources on aerosol size distribution*

Aerosol size distribution is a key parameter in describing light extinction for cloud-free conditions. Aerosols with a diameter range of 0.1–1.0 μm, corresponding to the accumulation mode, scatter light most efficiently (Seinfeld and Pandis, 2006). The effects of the three additional HONO sources on N_a over different size bins are shown in Fig. 8a. Aerosols within the diameter range of 0.078–1.25 μm (covering 2–5 bins) showed significant enhancements, indicating that additional HONO sources can increase the accumulation mode number concentrations (AMNC). The N_a enhancements for 2–5 bins were 9.0%, 4.1%, 8.5%, and 1.2%, respectively.

Elshorbany et al. (2014) showed that elevated HONO concentrations can produce significantly higher particle number concentrations in both the hydrophilic accumulation mode and the hydrophilic Aitken mode. In the present study, however, N_a in the Aitken mode (1st bin with particle diameters 0.039–0.078 μm; Table 1) were reduced by up to 26% when the additional HONO sources were included. This may be attributable mainly to the condensation and hydrolysis of the enhanced gas-phase HNO_3 and H_2SO_4 (Figs.7f and h) as well as the coagulation of the soluble new aerosol particles in the Aitken mode, and this finally resulted in the enhancements of AMNC. Elshorbany et al. (2014) also showed that enhanced HONO induces the transfer from hydrophobic to hydrophilic aerosol modes, which is mainly related to the condensation of H_2SO_4 on the hydrophobic particles. For example, over eastern China the particle number concentration in the hydrophobic Aitken mode is reduced on average by

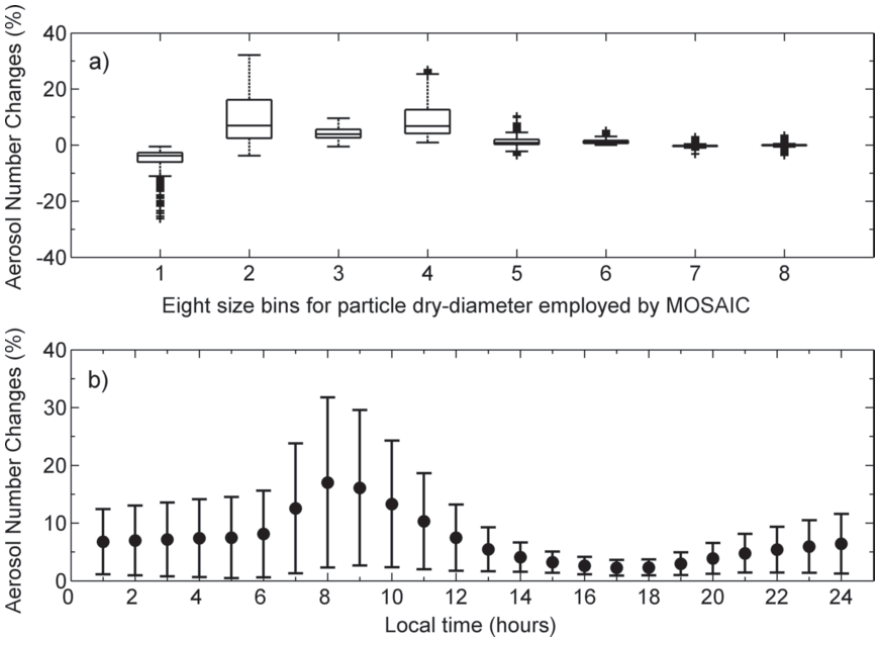

Fig. 8. Monthly-mean aerosol number (N_a) enhancements spatially averaged over the NCP in August 2007 due to the inclusion of additional HONO sources. (a) Box and whisker plots of aerosol number concentration enhancements for the eight diameter size bins shown in Table 1. For each box, the central mark is the median; the upper and lower edges of the box are the 25th and 75th percentiles, respectively; the whiskers extend to the most extreme data points not considered outliers; and outliers are plotted individually. (b) Averaged diurnal variation of increases in N_a with aerosol diameter in the range of 0.08–1.25 μm, which corresponds to the bins from the 2nd to 5th set by MOSAIC. Error bars are the standard deviations.

~6%, while that of the hydrophilic accumulation mode is enhanced by 14% (Elshorbany et al., 2014). Therefore, the enhanced aerosol hygroscopicity due to the additional HONO sources may also contribute to the AMNC enhancements, and this will be studied in future work by differentiating the aerosol size distribution in the WRF/Chem model into the hydrophilic and hydrophobic modes.

Figure 8b shows the averaged diurnal variation of AMNC enhancements. Because HONO photolysis is one of the most significant sources of OH in the early morning (Alicke et al., 2002), AMNC enhancements due to the three additional HONO sources were larger in the morning and peaked at 0800 LST, corresponding to high HONO concentrations during that period (Fig. 5a). The AMNC enhancements during the night were mainly related to the NO_2 heterogeneous reaction on aerosol surfaces, which produces NO_3^- in the presence of NH_3. Figure 8 suggests that HONO sources can cause decreases in visibility via increasing AMNC.

The spatial distribution of increases in monthly-mean N_a in the range of 2–5 bins is shown in Fig. 9a. The additional HONO sources increased AMNC in extended areas of the NCP, especially for regions with high emissions of NO_x, e.g., Beijing, Tianjin and Shijiazhuang. In those big cities, 15%–20% enhancements were found for AMNC. Among the three additional HONO sources, the NO_2 heterogeneous reaction occurring on aerosol surfaces was the largest contributor for increasing AMNC (by 5%–15%). During summer, aerosol hygroscopic growth with increasing RH results in an increase of aerosol size and a decrease of the real part of the aerosol refractive index (Yoon and Kim, 2006; Pan et al., 2009; Chen et al., 2012). Shown in Fig. 9b are the enhancements of monthly-mean S_a in the range of 2–5 bins due to the additional HONO sources. Similar to Fig. 9a, the accumulation mode S_a also increased by up to 10%–20% in polluted areas.

3.3. *Conceptual model for the impacts of additional HONO sources on visibility*

A conceptual model (Fig. 10) is proposed to describe how the additional HONO sources impact atmospheric visibility prediction. The impact of HONO sources on the air quality is more significant in polluted areas than in rural or background regions (Sarwar et al., 2009; Li et al., 2011; Jorba et al., 2012; An et al., 2013). When HONO concentrations increase in the atmosphere, OH is additionally produced by HONO photolysis. For instance, monthly-mean daytime OH concentrations increase by up to 84% over the NCP when the additional HONO sources are considered in the WRF/Chem model (An et al., 2013). The NO_2^* chemistry not only produces OH directly, but also enhances OH production from other formation pathways, e.g., the HONO photolysis and the reaction of NO with HO_2 (Sarwar et al., 2009). Monthly mean daytime OH concentrations increase by up to 21% in the eastern U.S. and 28% in the western U.S. due to NO_2^* chemistry. The enhanced OH concentrations contribute to more O_3 production from the catalytic oxidation of volatile organic compounds (VOCs) when NO_x is present. Photolysis of the increased O_3 can further produce OH, which can oxidize NO_2 and SO_2 in the presence of NH_3 to produce sulfate and nitrate. Furthermore, OH enhancements also lead to more H_2O_2 production (Fig. 7g), which contributes to sulfate formation through the aqueous phase oxidation.

Both SO_4^{2-} and NO_3^- are the dominant contributors to the total extinction parameter in many regions of the world, e.g., the eastern coast of the U.S. (Debell et al., 2006), Beijing and the Pearl River Delta region of China (Cheung et al., 2005; Jung et al., 2009), and northwest England (Colbeck and Har-

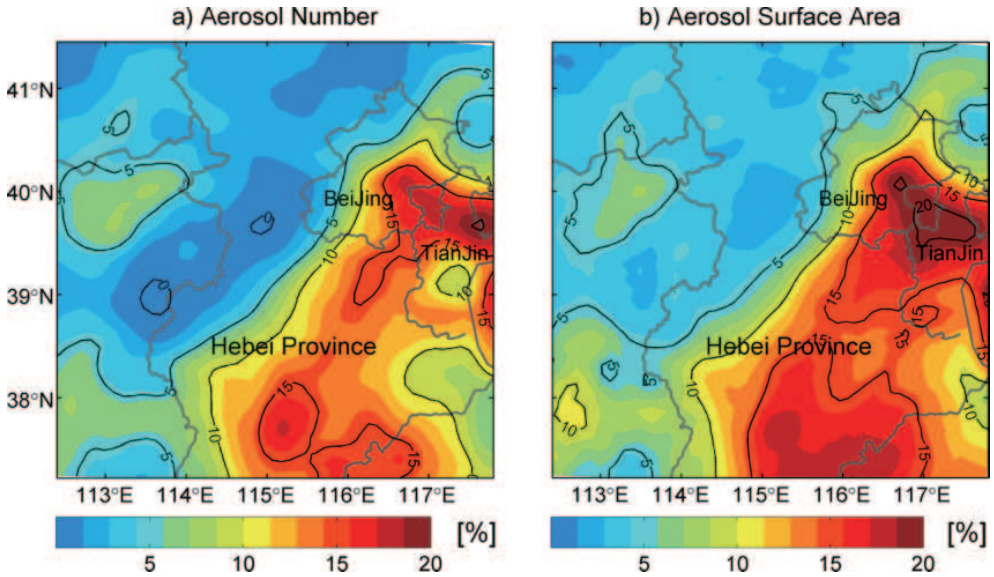

Fig. 9. Percentage increases of monthly mean (a) aerosol number and (b) aerosol surface area in the 2nd–5th diameter size bins over the NCP in August 2007 due to the inclusion of NO_2^* chemistry, the NO_2 heterogeneous reaction on aerosol surfaces, and HONO emissions. The aerosol diameter size bins are shown in Table 1.

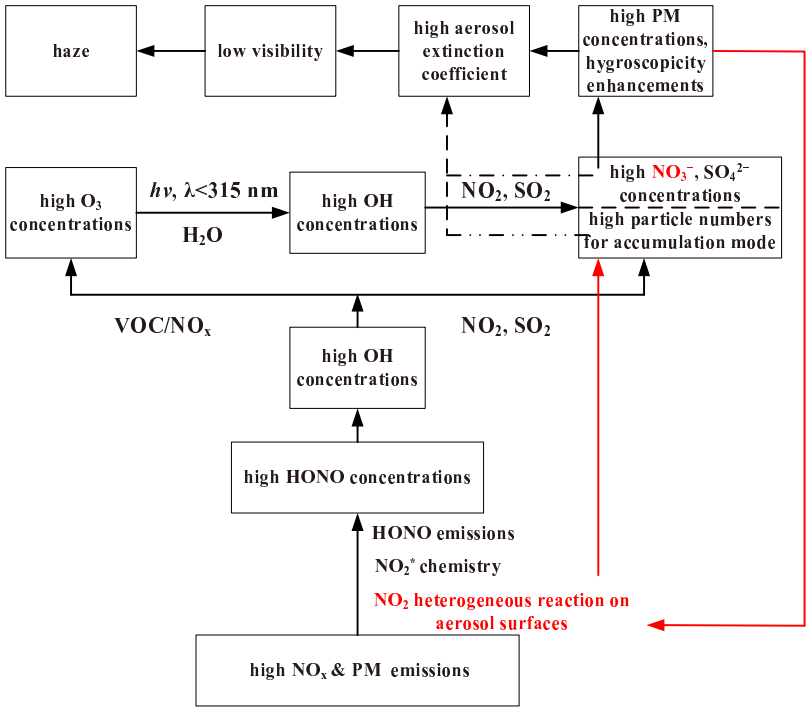

Fig. 10. A proposed conceptual model for the effects of additional HONO sources on visibility and haze.

rison, 1984). Increased NO_3^- and SO_4^{2-} can lead to $PM_{2.5}$ enhancements, and increase aerosol hygroscopicity, which result in high aerosol extinction estimations. Furthermore, the three additional HONO sources, especially the NO_2 heterogeneous reaction occurring on aerosol surfaces, can induce high aerosol numbers in the accumulation mode. In this mode, aerosols scatter light most efficiently. It is emphasized that the NO_2 heterogeneous reaction as a positive feedback mechanism enhances the conversion of primary gas pollutants to secondary aerosols. Shown as red lines in Fig. 10, the heterogeneous reaction increases aerosol number concentrations and NO_3^- concentrations. These further increase the surface area of aerosols affecting heterogeneous reactions, which lead to the conversion of primary pollutants to secondary pollutants.

In summary, increases in concentrations of $PM_{2.5}$, its hydrophilic components, and aerosol numbers in the accumulation mode due to the additional HONO sources reduce visibility significantly, and this may result in more favorable haze formation conditions under stagnant meteorological situations. The basic reason for the visibility impairment due to the additional HONO sources is that the additional HONO sources lead to the enhancements in the concentrations of oxidants (OH, H_2O_2 and O_3), which subsequently enhance the atmospheric oxidizing capacity. It should be noted that, in this study, both rainy and foggy days were excluded from the analysis. Previous observations show that AMNC presents a close relationship with cloud droplet number concentration (CNDC) (Hegg et al., 2012). As a result, the enhanced AMNC due to the additional HONO sources may increase CNDC during foggy days, which can further reduce visibility, but this was not studied here.

4. Conclusions

Three additional HONO sources (NO_2^* chemistry, the NO_2 heterogeneous reaction on aerosol surfaces, and HONO emissions) were added into a fully coupled meteorology–chemistry numerical forecasting model to investigate the impacts of the increased HONO concentrations on visibility over the NCP during August 2007. The main conclusions of the study can be summarized as follows:

(1) The spatial pattern and diurnal variations of visibility were generally reproduced well by the WRF/Chem model over the NCP, except that an overestimation was found in the southern NCP region.

(2) The three additional HONO sources exerted a significant effect on visibility estimation. The largest decreases in *Vis* at 1400 LST during August 2007 were about 40%–55% over Bohai Bay, 20%–30% (3–4 km) in local urban areas, and 10% (1–2 km) in rural areas.

(3) Among the three HONO sources, the NO_2 heterogeneous reaction was the largest contributor to the visibility decrease. Monthly mean total aerosol extinction coefficients were increased by 10%–21% in most areas of the NCP due to the additional HONO sources.

(4) The three HONO sources reduced visibility through enhancing aerosol concentrations, particularly for hydrophilic components. Monthly mean concentrations of NO_3^-, NH_4^+, SO_4^{2-} and $PM_{2.5}$ were increased by 20%–52% (3–11 μg m^{-3}), 10%–38%, 6%–10%, and 6%–11% (9–17 μg m^{-3}) in urban areas of the NCP, respectively. Increases

in daily mean concentrations of NO_3^- and NH_4^+ were up to approximately 100% during August 2007.

(5) The additional HONO sources caused visibility degradation via increasing accumulation-mode aerosol numbers and surface areas. Monthly-mean AMNC values were enhanced by 15%–20% in large areas of the NCP because of these sources. Accordingly, S_a in the accumulation mode was increased by 10%–20%.

(6) A conceptual model of the effects of HONO sources on visibility was proposed and the effect of the NO_2 heterogeneous reaction as a positive feedback mechanism that enhances the conversion of primary gas pollutants to secondary aerosols was also emphasized.

Overall, the results suggest that visibility estimation in forecasting models should consider the enhanced atmospheric oxidizing capacity due to additional HONO sources, especially in areas with high concentrations of NO_x and aerosols.

Acknowledgements. This research was supported by the Beijing Natural Science Foundation (Grant No. 8144054), the Key Project of the Chinese Academy of Sciences (Grant No. XDB05030301), the National Natural Science Foundation of China (Grant No. 41175105), and the Carbon and Nitrogen Cycle project of the Institute of Atmospheric Physics, Chinese Academy of Sciences. Special thanks are given to Prof. XIE Pinhua from Anhui Institute of Optics and Fine Mechanics, Chinese Academy of Sciences, for providing HONO observations in Beijing, and Prof. WANG Yuesi from CERN, LAPC, Institute of Atmospheric Physics, Chinese Academy of Sciences, for offering observed data of O_3, $PM_{2.5}$, and PM_{10}. Thanks are also extended to the anonymous reviewers for key suggestions that helped improve the manuscript.

REFERENCES

Ackerman, T. P., and O. B. Toon, 1981: Absorption of visible radiation in atmosphere containing mixtures of absorbing and nonabsorbing particles. *Appl. Opt.*, **20**, 3661–3667.

Alicke, B., U. Platt, and J. Stutz, 2002: Impact of nitrous acid photolysis on the total hydroxyl radical budget during the Limitation of Oxidant Production/Pianura Padana Produzione di Ozono study in Milan. *J. Geophys. Res.*, **107**(D22), 8196, doi: 10.1029/2000JD000075.

Amedro, D., A. E. Parker, C. Schoemaecker, and C. Fittschen, 2011: Direct observation of OH radicals after 565 nm multiphoton excitation of NO_2 in the presence of H_2O. *Chem. Phys. Lett.*, **513**, 12–16.

An, J., Y. Li, F. Wang, and P. Xie, 2011: Impacts of photoexcited NO_2 chemistry and heterogeneous reactions on concentrations of O_3 and NO_y in Beijing, Tianjin and Hebei Province of China. *Air Quality-Models and Applications*, N. Mazzeo, Ed., InTech, 197–210.

An, J., Y. Li, Y. Chen, J. Li, Y. Qu, and Y. Tang, 2013: Enhancements of major aerosol components due to additional HONO sources in the North China Plain and implications for visibility and haze. *Adv. Atmos. Sci.*, **30**, 57–66, doi: 10.1007/s00376-012-2016-9.

Barnard, J., J. Fast, G. Paredes-Miranda, W. Arnott, and A. Laskin, 2010: Technical note: Evaluation of the WRF-Chem "aerosol chemical to aerosol optical properties" module using data from the MILAGRO campaign. *Atmos. Chem. Phys.*, **10**, 7325–7340.

Cao, J., and Coauthors, 2012: Impacts of aerosol compositions on visibility impairment in Xi'an, China. *Atmos. Environ.*, **59**, 559–566.

Chang, D., Y. Song, and B. Liu, 2009: Visibility trends in six megacities in China 1973–2007. *Atmospheric Research.*, **94**, 161–167.

Chen, J., and Coauthors, 2012: A parameterization of low visibilities for hazy days in the North China Plain. *Atmos. Chem. Phys.*, **12**, 4935–4950.

Cheng, Y., J. Heintzenberg, B. Wehner, Z. Wu, H. Su, M. Hu, and J. Mao, 2008: Traffic restrictions in Beijing during the Sino-African Summit 2006: Aerosol size distribution and visibility compared to long-term *in situ* observations. *Atmos. Chem. Phys.*, **8**, 7583–7594.

Cheung, H. C., T. Wang, K. Baumann, and H. Guo, 2005: Influence of regional pollution outflow on the concentrations of fine particulate matter and visibility in the coastal area of southern China. *Atmos. Environ.*, **39**, 6463–6474.

Colbeck, I., and R. M. Harrison, 1984: Ozone-secondary aerosol-visibility relationships in North-West England. *Sci. Total Environ.*, **34**, 87–100.

Crowley, J. N., and S. A. Carl, 1997: OH formation in the photoexcitation of NO_2 beyond the dissociation threshold in the presence of water vapor. *J. Phys. Chem.* (*A*)., **101**, 4178–4184.

Debell, L. J., K. A. Gebhart, W. C. Malm, M. L. Pitchford, B. A. Schichtel, and W. H. White, 2006: Spatial and seasonal patterns and temporal variability of hazy and its constituents in the United States: Report IV. [Available online at http://vista.cira.colostate.edu/improve/publications/ Reports/ 2006/ 2006.htm.]

Deng, J. J., T. J. Wang, Z. Q. Jiang, M. Xie, R. J. Zhang, X. X. Huang, and J. L. Zhu, 2011: Characterization of visibility and its affecting factors over Nanjing, China. *Atmospheric Research*, **101**, 681–691.

Elshorbany, Y. F., P. J. Crutzen, A. Pozzer, H. Tost, and J. Lelieveld, 2014: Global and regional impacts of HONO on the chemical composition of clouds and aerosols. *Atmos. Chem. Phys.*, **14**, 1167–1184.

Emmons, L. K., and Coauthors, 2010: Description and evaluation of the model for ozone and related chemical tracers, version 4 (MOZART-4). *Geosci. Model. Dev.*, **3**, 43–67.

Ensberg, J. J., M. Carreras-Sospedra, and D. Dabdub, 2010: Impacts of electronically photo-excited NO_2 on air pollution in the South Coast Air Basin of California. *Atmos. Chem. Phys.*, **10**, 1171–1181.

Fast, J. D., and Coauthors, 2006: Evolution of ozone, particulates, and aerosol direct radiative forcing in the vicinity of Houston using a fully coupled meteorology-chemistry-aerosol model. *J. Geophys. Res.*, **111**, 1–29.

Finlayson-Pitts, B., L. Wingen, A. Sumner, D. Syomin, and K. Ramazan, 2003: The heterogeneous hydrolysis of NO_2 in laboratory systems and in outdoor and indoor atmospheres: An integrated mechanism. *Phys. Chem. Chem. Phys.*, **5**, 223–242.

Gonçalves, M., D. Dabdub, W. L. Chang, O. Jorba, and J. M. Baldasano, 2012: Impact of HONO sources on the performance of mesoscale air quality models. *Atmos. Environ.*, **54**, 168–176.

Grell, G. A., S. E. Peckham, R. Schmitz, S. A. McKeen, G. Frost,

W. C. Skamarock, and B. Eder, 2005: Fully coupled "online" chemistry within the WRF model. *Atmos. Environ.*, **39**, 6957–6975.

Gultepe, I., M. D. Müller, and Z. Boybeyi, 2006: A new visibility parameterization for warm-fog applications in numerical weather prediction models. *J. Appl. Meteor. Climatol.*, **45**, 1469–1480.

Gultepe, I., and Coauthors, 2007: Fog research: A review of past achievements and future perspectives. *Pure Appl. Geophys.*, **164**, 1121–1159.

Gultepe, I., J. Milbrandt, S. Benjamin, G. A. Isaac, S. G. Cober, and B. Hansen, 2008: Visibility parameterization for forecasting model applications. *Proceedings of the* 15*th International Conference on Clouds and Precipitation* (*ICCP*), Cancun, Mexico.

Gultepe, I., and Coauthors, 2009: The fog remote sensing and modeling field project. *Bull. Amer. Meteor. Soc.*, **90**, 341–359.

Gutzwiller, L., F. Arens, U. Baltensperger, H. W. Gaggeler, and M. Ammann, 2002: Significance of semivolatile diesel exhaust organics for secondary HONO formation. *Environ. Sci. Technol.*, **36**, 677–682.

Han, X., M. G. Zhang, J. H. Tao, L. L. Wang, J. Gao, S. L. Wang, and F. Chai, 2013: Modeling aerosol impacts on atmospheric visibility in Beijing with RAMS-CMAQ. *Atmos. Environ.*, **72**, 177–191.

Hegg, D. A., D. S. Covert, H. H. Jonsson, and R. K. Woods, 2012: A simple relationship between cloud drop number concentration and precursor aerosol concentration for the regions of Earth's large marine stratocumulus decks. *Atmos. Chem. Phys.*, **12**, 1229–1238.

Ianniello, A., F. Spataro, G. Esposito, I. Allegrini, M. Hu, and T. Zhu, 2011: Chemical characteristics of inorganic ammonium salts in $PM_{2.5}$ in the atmosphere of Beijing (China). *Atmos. Chem. Phys.*, **11**, 10 803–10 822.

Jacob, D. J., 2000: Heterogeneous chemistry and tropospheric ozone. *Atmos. Environ.*, **34**, 2131–2159.

Jorba, O., and Coauthors, 2012: Potential significance of photoexcited NO_2 on global air quality with the NMMB/BSC chemical transport model. *J. Geophys. Res.*, **117**(D13301), doi: 10.1029/2012JD017730.

Jung, J., H. Lee, Y. J. Kim, X. Liu, Y. Zhang, M. Hu, and N. Sugimoto, 2009: Optical properties of atmospheric aerosols obtained by in situ and remote measurements during 2006 Campaign of Air Quality Research in Beijing (CAREBeijing-2006). *J. Geophys. Res.*, **114**(D00G02), doi: 10.1029/2008JD010337.

Kleffmann, J., K. Becker, and P. Wiesen, 1998: Heterogeneous NO_2 conversion processes on acid surfaces: possible atmospheric implications. *Atmos. Environ.*, **32**, 2721–2729.

Koschmieder, H., 1924: Theorie der horizontalen sichtweite. *Beitr. Phys. Freien Atmos.*, **12**, 33–53.

Kurtenbacha, R., and Coauthors, 2001: Investigations of emissions and heterogeneous formation of HONO in a road traffic tunnel. *Atmos. Environ.*, **35**, 3385–3394.

Li, G., W. Lei, M. Zavala, R. Volkamer, S. Dusanter, P. Stevens, L. Molina, 2010: Impacts of HONO sources on the photochemistry in Mexico City during the MCMA-2006/MILAGO Campaign. *Atmos. Chem. Phys.*, **10**, 6551–6567.

Li, S., J. Matthews, and A. Sinha, 2008: Atmospheric hydroxyl radical production from electronically excited NO_2 and H_2O. *Science*, **319**, 1657–1660.

Li, Y., J. An, M. Min, W. Zhang, F. Wang, and P. Xie, 2011: Impacts of HONO sources on the air quality in Beijing, Tianjin and Hebei Province of China. *Atmos. Environ.*, **45**, 4735–4744.

Lin, M., J. Tao, C. Y. Chan, J. J. Cao, Z. S. Zhang, L. H. Zhu, and R. J. Zhang, 2012: Regression analyses between recent air quality and visibility changes in megacities at four haze regions in China. *Aerosol and Air Quality Research*, **12**, 1049–1061.

Mebust, M. R., B. K. Eder, F. S. Binkowski, and S. J. Roselle, 2003: Models-3 Community Multiscale Air Quality (CMAQ) model aerosol component 2. Model evaluation. *J. Geophys. Res.*, **108**(D6), 4184, doi: 10.1029/2001JD001410.

Pan, X., P. Yan, J. Tang, J. Ma, Z. Wang, A. Gbaguidi, and Y. Sun, 2009: Observational study of influence of aerosol hygroscopic growth on scattering coefficient over rural area near Beijing mega-city. *Atmos. Chem. Phys.*, **9**, 7519–7530.

Quan, J., Q. Zhang, H. He, J. Liu, M. Huang, and H. Jin, 2011: Analysis of the formation of fog and haze in North China Plain (NCP). *Atmos. Chem. Phys.*, **11**, 8205–8214.

Sarwar, G., R. W. Pinder, K. W. Appel, R. Mathur, and A. G. Carlton, 2009: Examination of the impact of photoexcited NO_2 chemistry on regional air quality. *Atmos. Environ.*, **43**, 6383–6387.

Seinfeld, J. H., and S. N. Pandis, 2006: *Atmos. Chem. Phys.: From Air Pollution to Climate Change*. 2nd ed., Wiley, 1232 pp.

Tang, Y., J. An, Y. Li, and F. Wang, 2014: Uncertainty in the uptake coefficient for HONO formation on soot and its impacts on concentrations of major chemical components in the Beijing-Tianjin-Hebei region. *Atmos. Environ.*, **84**, 163–171.

Wennberg, P. O., and D. Dabdub, 2008: Rethinking ozone production. *Science*, **319**, 1624–1625.

Yang, F., J. Tan, Q. Zhao, Z. Du, K. He, Y. Ma, F. Duan, and G. Chen, 2011: Characteristics of $PM_{2.5}$ speciation in representative megacities and across China. *Atmos. Chem. Phys.*, **11**, 5207–5219.

Yoon, S.-C., and J. Kim, 2006: Influences of relative humidity on aerosol optical properties and aerosol radiative forcing during ACE-Asia. *Atmos. Environ.*, **40**, 4328–4338.

Zaveri, R. A., and L. K. Peters, 1999: A new lumped structure photochemical mechanism for large-scale applications. *J. Geophys. Res.*, **104**(D23), 30 387—30 415.

Zaveri, R. A., R. C. Easter, J. D. Fast, and L. K. Peters, 2008: Model for Simulating Aerosol Interactions and Chemistry (MOSAIC). *J. Geophys. Res.*, **113**(D13204), doi: 10.1029/2007JD008782.

Zhang, Q., and Coauthors, 2009: Asian emissions in 2006 for the NASA INTEX-B mission. *Atmos. Chem. Phys.*, **9**, 5131–5153.

Zhang, Q. H., J. P. Zhang, and H. W. Xue, 2010: The challenge of improving visibility in Beijing. *Atmos. Chem. Phys.*, **10**, 7821–7827.

Zhang, R., G. Sarwar, J. C. H. Fung, and A. H. K. Lau, 2013: Role of photoexcited nitrogen dioxide chemistry on ozone formation and emission control strategy over the Pearl River Delta, China. *Atmospheric Research*, **132–133**, 332–344.

Zhao, C., and Coauthors, 2006: Aircraft measurements of cloud droplet spectral dispersion and implications for indirect aerosol radiative forcing. *Geophys. Res. Lett.*, **33**, L16809, doi: 10.1029/2006GL026653.

Zhu, Y. W., and Coauthors, 2009: Observational study of atmospheric HONO in summer of Beijing. *Environ. Sci.*, **30**, 1567–1573.